

Electrochemical performance of silicon thin film anodes covered by diamond-like carbon with various surface coating morphologies

Sang-Ok Kim · Heung-Taek Shim · Joong Kee Lee

Received: 23 June 2009 / Revised: 25 August 2009 / Accepted: 27 August 2009 / Published online: 18 September 2009
© Springer-Verlag 2009

Abstract Four different kinds of diamond-like carbon (DLC) coating morphologies on the surface of silicon films were prepared directly on a copper foil by using radio frequency plasma-enhanced chemical vapor deposition at 200°C. A thin double layer film consisting of DLC (60 nm) and silicon film (250 nm) was fabricated for use as the anode material of lithium secondary batteries, and its electrochemical performance was also examined with special attention being paid to the surface coverage of the DLC film. The full coverage of silicon by the DLC film resulted in poor capacity due to the ensuing low reactivity with the lithium ions. On the other hand, the partial coating of the DLC film on the silicon film not only reduced the capacity fading, but also increased the discharge capacity during the charge/discharge cycles. These results indicated that the good dispersion of the DLC coating, obtained by using a smaller coating sector on the silicon film, improved the integrity of the electrode structure, thus giving higher capacities and reduced capacity fading.

Keywords Thin films · PECVD · Coatings · Electrochemical properties

Introduction

Due to the rapid progress of information technology, consumer electronics devices such as cellular phones and laptops require lithium ion batteries (LIBs) with a high energy density, high power density, high efficiency, and light weight. In this regard, considerable efforts have been made to improve the performance of LIBs. For the anode materials, systems based on metals such as silicon [1–3] and tin [4–6] have been studied as alternative candidates, due to their very high theoretical capacities in comparison with the conventional graphite materials (theoretical capacity of 372 mA h g⁻¹). Silicon is of great interest because it can react with lithium to form binary alloys with a maximum lithium uptake of 4.4 atoms per Si atom, namely, Li₂₂Si₅ [7, 8]. In the case of Li₂₂Si₅, the theoretical specific capacity is 4,200 mA h g⁻¹, which is the highest capacity for any of the Li alloys studied to date [9]. However, the enormous volume change during the alloying/dealloying process of lithium ions with silicon causes the rapid disintegration of the electrode and results in severe capacity fading. This means that the volume variation of silicon causes serious problems, such as the breaking of the crystallite particles to form an amorphous phase [10] and the loss of contact between the silicon thin film and copper substrate which can lead to poor cycle performance [11].

It is believed that the characteristics of the solid electrolyte interphase (SEI) film at the surface of the silicon layer play an important role in the reversible charge/discharge reaction [7, 8]. Because the continuous formation of the SEI film due to the direct contact with the electrolyte leads to the instability of the interfacial properties, further studies on the interfacial phenomena between the electrode and the electrolyte solution are needed [12, 13].

In this research, in order to improve the electrochemical properties of the silicon anode in the liquid electrolyte, it was

S.-O. Kim · H.-T. Shim · J. K. Lee (✉)
Advanced Energy Materials Processing Laboratory,
Battery Research Center,
Korea Institute of Science and Technology,
P.O. Box 131, Cheongryang, Seoul 130-650, South Korea
e-mail: leejk@kist.re.kr

Present Address:

H.-T. Shim
SAMSUNG SDI CO., LTD,
428-5, Gongse-dong, Giheung-gu, Yongin-si,
Gyeonggi-do 446-577, South Korea

decided to focus on the interfacial reaction that affects the cycleability and overall lifetime of the lithium ion batteries. A diamond-like carbon (DLC) film is introduced as a coating material for the silicon anode to obtain a stable interface. DLC films have been extensively studied over the last few decades because of their unique microstructure consisting of sp^2 -bonded carbon clusters interconnected with sp^3 -bonded sites [14, 15], and their numerous interesting properties such as good hardness, high elasticity, low friction coefficient, chemical stability, and high electrical resistivity (approximately $10^{17} \Omega \text{ cm}$) [16–18]. It has been reported that the use of carbon films such as DLC [19–21] and fullerene (C_{60}) [22] can stabilize the interfacial properties of the active materials for LIBs. The purpose of this study is to investigate the effect of the geometric design of the electrode on the electrochemical performance of a silicon thin film cell. It was expected that the geometric design of the thin film anode material through the use of a DLC coating on the silicon electrode would give rise to the necessary high capacity along with good cyclic performance.

Experimental

Two kinds of thin films were deposited by gas phase reactions using the plasma-enhanced chemical vapor deposition (PECVD) method. Figure 1 shows a schematic diagram of the PECVD system used for our depositions. Silicon thin films were deposited on a copper foil (18 μm thick) substrate which serves as a current collector, using a mixture gas of

argon and silane (SiH_4). The deposition parameters are shown in Table 1. The base pressure was 1.0×10^{-4} Torr, and the working pressure was 5.0×10^{-2} Torr. During the deposition, the radio frequency (RF) power was maintained at 200 W for 30 min, and the substrate temperature was kept at 200°C . The deposition of the DLC films on the silicon anode was carried out using the following procedure. Table 1 also presents the deposition conditions of the DLC film. The self-bias produced on the substrate was approximately -300 V . A mixture of acetylene (C_2H_2), hydrogen, and argon was used as the processing gas. The gas flow rates of argon, hydrogen, and acetylene were 10, 20, and 5 sccm, respectively, and the RF power was 120 W at a working pressure of 0.1 Torr. Four different kinds of DLC-coated silicon electrodes were prepared to investigate the relationship between the surface morphology and their electrochemical performance. In this work, the different surface coating morphologies were prepared by a masking method. A stainless steel plate ($2 \times 1 \text{ cm}^2$) and two types of stainless steel mesh ($2 \times 2 \text{ cm}^2$) were placed onto the silicon thin film anode. Subsequently, carbon film was deposited for 5 min at 200°C . As can be seen in Table 2, S0 stands for the pure silicon electrode without any treatment, S1 represents the silicon electrode with DLC coated over its entire surface, S2 represents the silicon electrode with DLC coated over half of its surface, S3 represents the silicon electrode partially coated with DLC film where the dimensions of each DLC coating sector were $1.5 \times 1.5 \text{ mm}^2$, and S4 also represents the silicon electrode partially coated with DLC film, but the dimensions of each DLC-coating sector were $300 \times 300 \mu\text{m}^2$.

Half cells were used to examine the electrochemical performance of the DLC-coated silicon thin films. The DLC-coated silicon thin film was employed as a working

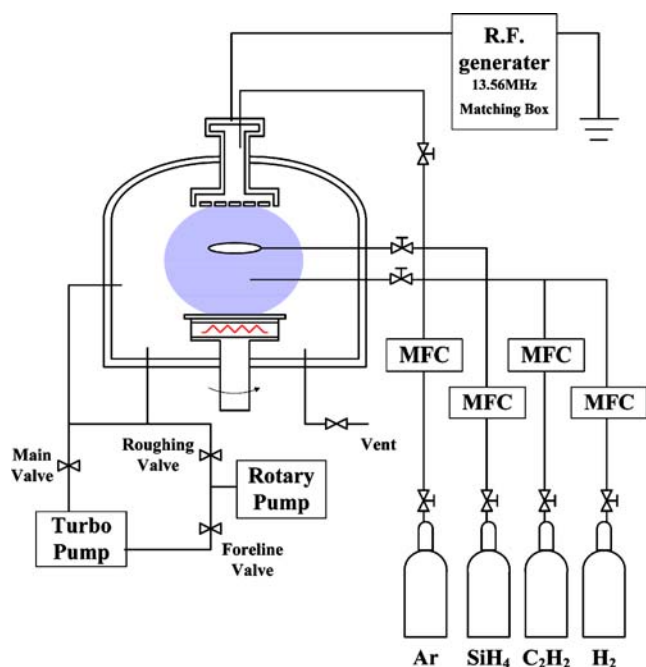



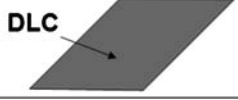
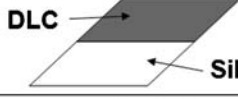
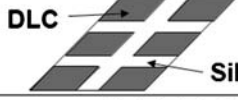
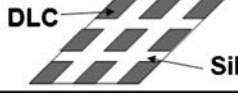
Fig. 1 Schematic diagram of PECVD system

Table 1 The conditions used for the silicon thin film deposition and DLC-coating procedures

Process parameter	Condition	
	DLC	Silicon
Material	DLC	Silicon
RF power (W)	120	200
Base pressure (Torr)	1.0×10^{-4}	1.0×10^{-4}
Working pressure (Torr)	1.0×10^{-1}	5.0×10^{-2}
Ar flow rate (sccm)	10	50
SiH_4 flow rate (sccm)	–	15
C_2H_2 flow rate (sccm)	5	–
H_2 flow rate (sccm)	20	–
Substrate temperature ($^\circ\text{C}$)	200	200
Reaction time (min)	5	30
Thickness (nm)	60	250

DLC diamond-like carbon, RF radio frequency

Table 2 Explanation of DLC-coating morphology on the surface of the silicon thin film

Sample name	Sample condition	Surface shape
S0	Silicon thin film electrode without DLC coating	 Silicon
S1	DLC coating on the whole area of silicon electrode	 DLC
S2	DLC coating on the half area of silicon electrode	 DLC Silicon
S3	Partial coating of DLC on silicon electrode (The dimension of each DLC coating sector is $1.5 \times 1.5 \text{ mm}^2$)	 DLC Silicon
S4	Partial coating of DLC on silicon electrode (The dimension of each DLC coating sector is $300 \times 300 \text{ }\mu\text{m}^2$)	 DLC Silicon

electrode ($2 \times 2 \text{ cm}^2$), and a lithium foil was used as a counter electrode. The separator was a polypropylene microporous membrane, and the liquid electrolyte was 1 M LiPF_6 dissolved in a mixture of ethylene carbonate (EC), diethyl carbonate (DEC), and dimethyl carbonate (DMC; 1:1:1 in vol%). The half cells were fabricated and sealed in a dry room whose moisture content was maintained at less than 0.3%. Won A Tech (WBCS3000) and MACCOR (series-4000) testing systems were used for the galvanostatic charge–discharge cycling tests. All cells were cycled at a constant current of $100 \text{ }\mu\text{A cm}^{-2}$ at room temperature. Charge–discharge cycling tests were performed with cut-off voltages between 0.0 and 2.0 V (vs Li/Li^+).

Scanning electron microscopy (SEM), Raman, Fourier Transform Infrared (FT-IR), and X-ray photoelectron spectroscopy (XPS) analyses were carried out to characterize the properties of the deposited thin films. The surface morphology was investigated by SEM (HITACHI S-4100). The compositional and structural characterization of the DLC film was performed by Raman spectroscopy (Nicolet Almega XR Dispersive Raman Spectrometer, Thermo Electron Corporation), and Fourier transform infrared (Genesis Series FTIR Spectrometer, ATI Mattson) spectroscopy. In order to confirm the compositional changes after the electrochemical test, the electrode was investigated by XPS (Esca system, PHI-5800).

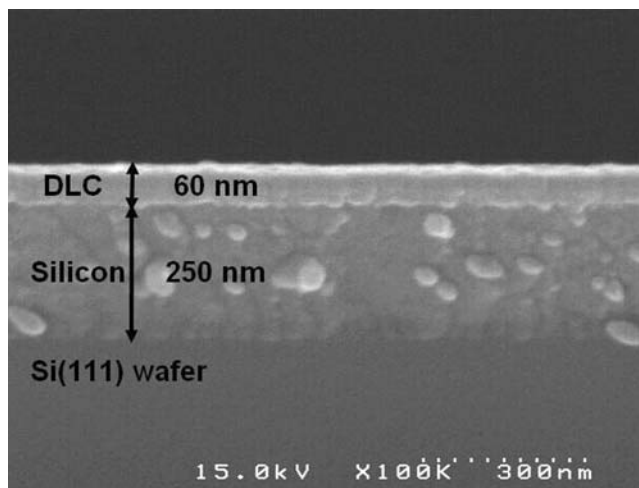


Fig. 2 SEM image of cross-sectional morphology of DLC-coated silicon thin film

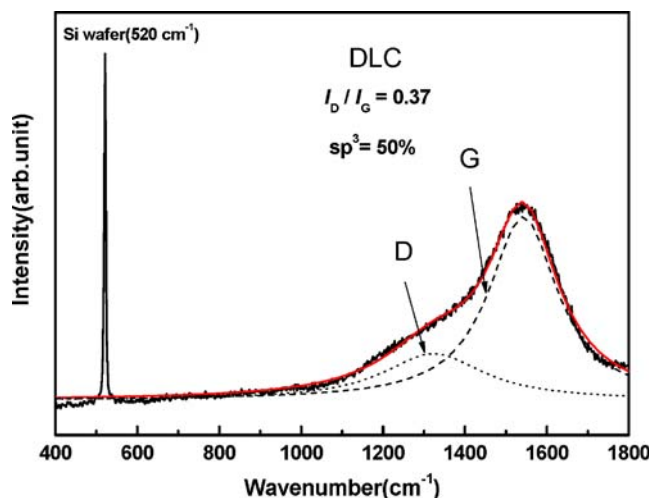


Fig. 3 Raman spectrum of DLC film prepared by radio frequency plasma-enhanced chemical vapor deposition (RF-PECVD)

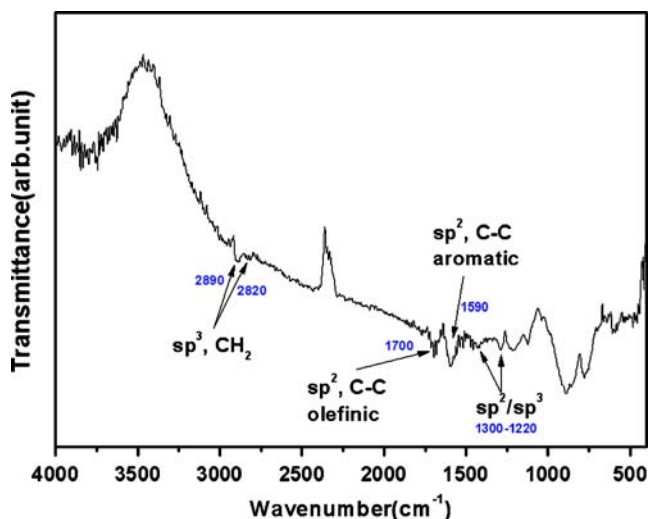


Fig. 4 FT-IR spectrum of DLC film deposited by RF-PECVD

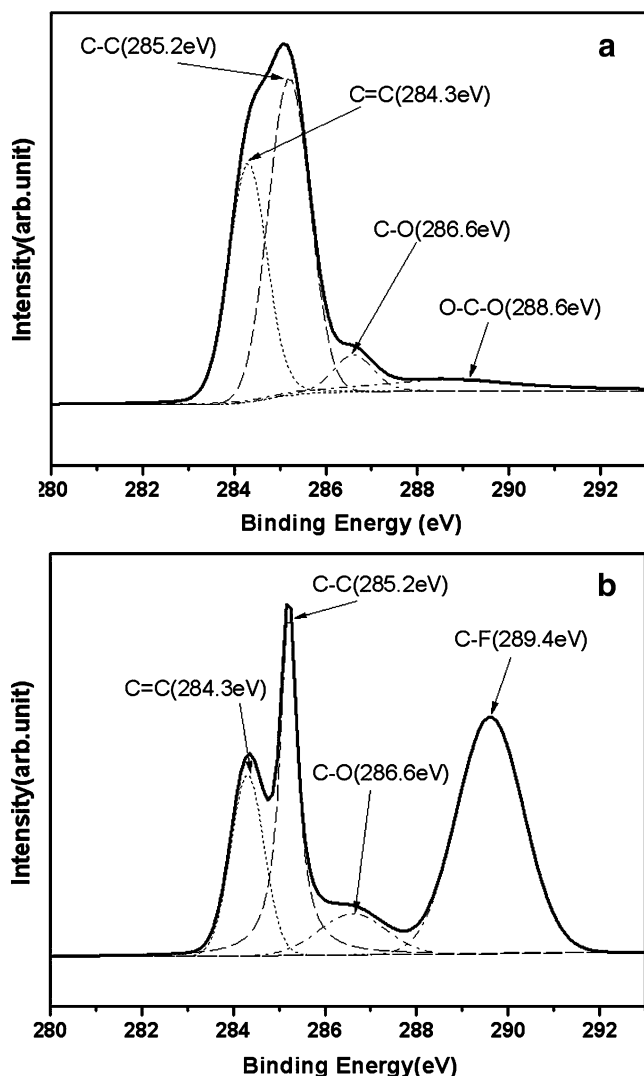


Fig. 5 The XPS narrow scan spectra before the electrochemical test (a) and after 40 cycles (b)

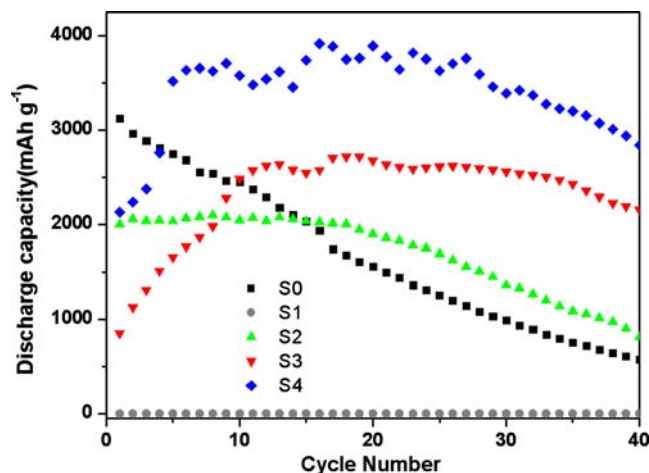


Fig. 6 Comparison of cycle performance for the DLC-coated Si electrodes with different surface morphologies. 1 M LiPF_6 EC + EMC + DMC (1:1:1 in v/v) electrolyte between 0.0–2.0 V at $100 \mu\text{A cm}^{-2}$. S1 whole area DLC coating, S2 half area DLC coating, S3 partial coating (coating sector is $1.5 \times 1.5 \text{ mm}^2$), S4 partial coating (coating sector is $300 \times 300 \mu\text{m}^2$)

Results and discussion

Scanning electron microscopy was employed to determine the cross-sectional thickness of the DLC and silicon films. As shown in Fig. 2, the top layer is the DLC, and the bottom layer is the silicon film. The total thickness is about 310 nm, which is composed of about 60 nm of DLC film and about 250 nm of silicon film.

Raman spectroscopy was employed to obtain the detailed bonding structure of the DLC film (Fig. 3). The Raman spectrum shows a strong band at 520 cm^{-1} corresponding to the crystalline silicon used as the substrate [23], strong broad peaks from 1,100 to 1,700 cm^{-1} and a weak shoulder peak at 1,200–1,400 cm^{-1} , which are characteristics of DLC [24]. The Raman spectrum of the DLC film can be deconvoluted into two peaks: the first peak at $1,580 \text{ cm}^{-1}$ assigned to the G band due to the sp^2 cluster configuration inside the film and the second peak at $1,350 \text{ cm}^{-1}$ assigned to the D band due to the disordered configuration of the grain boundaries. Quantitative analysis revealed that the intensity ratio of the D and G bands (I_D/I_G) was 0.37, and the sp^3 fraction was determined based on the dependence of this ratio (I_D/I_G) on the sp^3 contents in the DLC film taken from the literature. The obtained sp^3 content is approximately 50%. The increase of the H contents is closely related to the increase in the sp^3 fraction and lowering of the D peak. The Raman spectrum obtained in this experiment is typical characteristics of DLC.

As shown in Fig. 4, the presence of the sp^2 and sp^3 carbon sites is also observed in the FT-IR transmittance spectrum. The peaks of the transmittance spectra were found at $2,890 \text{ cm}^{-1}$ and $2,820 \text{ cm}^{-1}$, which are associated with the major presence of hydrogen in the form of sp^3

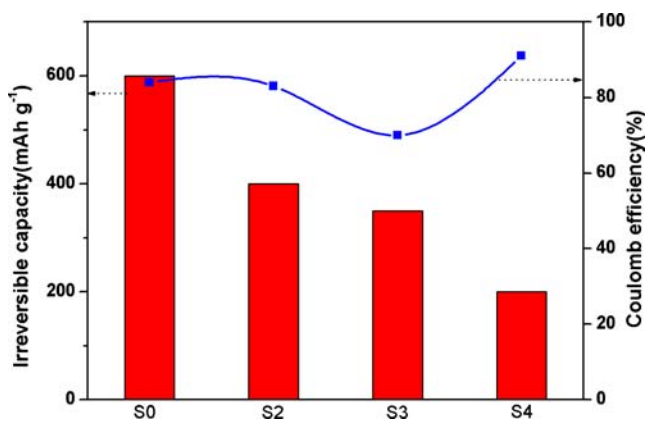


Fig. 7 Comparison of irreversible capacity and coulombic efficiency for different coating morphologies after the initial cycle. The electrochemical conditions and legends are as for Fig. 6

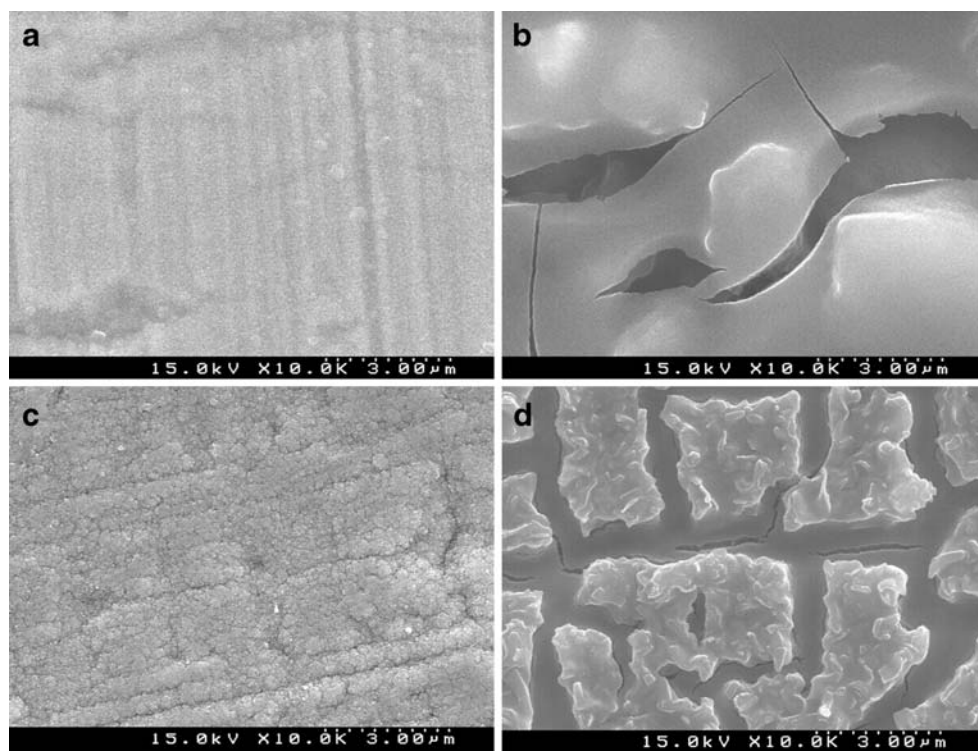
stretching asymmetry and symmetry modes, respectively. The peak at $1,700\text{ cm}^{-1}$ is due to the sp^2 olefinic C–C vibrational mode, and the peak at $1,590\text{ cm}^{-1}$ represents the sp^2 aromatic C–C vibrational mode. The wave numbers at $1,300\text{--}1,220\text{ cm}^{-1}$ are attributed to the C–C bending modes for both the sp^2 and sp^3 carbon [16, 25].

Figure 5 shows the change in the XPS spectrum before and after the electrochemical reaction on the natural surface of the DLC-coated silicon electrode (S4). Before the electrochemical test, this spectrum shows four components, namely peaks corresponding to the C=C bond at 284.3 eV, C–C bond at 285.2 eV, C–O bond at 286.6 eV, and O–C–O bond at 288.6 eV. Here, it is noted that the main component of the

surface consists of sp^2 and sp^3 which are the typical characteristics of DLC (see Fig. 5a). Figure 5b shows the XPS spectrum change after the 40th cycle. In this case, a new peak appears at 289.4 eV corresponding to the C–F bond. These results suggest that the DLC reacts with the electrolyte during the charge–discharge process. This means that the DLC films prevent the direct contact of the silicon electrode with the liquid electrolyte and consequently increase their stability [19–21].

The discharge capacities of the bare silicon and DLC coated silicon electrodes with different surface morphologies are given as a function of the cycle number in Fig. 6. According to the preliminary experiment, we could confirm that the silicon film deposited onto the copper substrate consisted of an almost completely amorphous phase. Thus, the theoretical density of amorphous silicon ($\sim 2.2\text{ g cm}^{-3}$) was applied to our experiment, and the loading mass of silicon on the copper substrate was calculated to be 0.055 mg cm^{-2} . Initially, the discharge capacity of the S0 electrode was about $3,122\text{ mA h g}^{-1}$, which is the highest capacity among the tested electrodes. However, it shows severe capacity fading in the subsequent cycles due to the large volume change during the charge–discharge reactions. In the case of the S1 electrode, no electrochemical reaction was observed, and the discharge capacity was zero during cycling. This may be due to the passivation effect of the DLC film, which hinders the lithium ion transfer through the DLC film [19–21]. The S2 electrode shows a relatively low capacity of $2,000\text{ mA h g}^{-1}$ at the first discharge

Fig. 8 Change in surface morphology between S0 and S4 before and after the electrochemical test. S0: before (a) and after 40 cycles (b), S4: before (c) and after 40 cycles (d)



reaction and then exhibits rather slow capacity fading during cycling, compared to the S0 electrode. On the other hand, the S3 and S4 electrodes display better discharge capacities and cycle performances than the other electrodes. The discharge capacity of the S3 electrode increases from $\sim 850 \text{ mA h g}^{-1}$ to $\sim 2,600 \text{ mA h g}^{-1}$ in the first ten cycles and remains above $2,200 \text{ mA h g}^{-1}$ until the 40th cycle. In the case of the S4 electrode, the discharge capacity also increases up to $\sim 3,700 \text{ mA h g}^{-1}$ in the first few cycles and shows stable cycle performance until the 40th cycle ($\sim 2,900 \text{ mA h g}^{-1}$). The capacity increase in the first ten cycles for the S3 and S4 electrodes is thought to be closely related to the lithium ion diffusion distance. Because the permeation of lithium ions through the DLC films is blocked, the active silicon coated by the DLC film cannot react with the lithium ions at the early stage. However, as the cycling proceeds, the DLC coated silicon is gradually exposed to the electrolyte, due to the volume change of the uncoated silicon, thus allowing the lithium ions to readily diffuse into the DLC-coated silicon region and enabling more silicon to participate in the lithium–silicon alloying/dealloying reactions. Hence, the discharge capacities of the S3 and S4 electrodes are increased in the first ten cycles. These results indicate that the well-dispersed DLC-coating sectors on the silicon electrode alleviate the mechanical stress on the active material during the repeated charge and discharge cycles and consequently enhance the cycle performance.

Figure 7 compares the irreversible capacity and coulombic efficiency of the four different surface morphologies after the initial cycle. According to Fig. 7, the surface coating morphology afforded by the DLC film strongly affects the electrochemical performance factors, such as the irreversible capacity and coulombic efficiency. The irreversible capacity of the S0 electrode after the first cycle is about 600 mA h g^{-1} , which is much higher than that of the S4 electrode (approximately 200 mA h g^{-1}). Also, the coulombic efficiency of the S4 electrode is over 90% in the first cycle. It is possible that the DLC films suppress the lithium ion diffusion, thereby causing the relatively low initial charge capacity of the S4 electrode. These results indicate that a smaller DLC coating sector on the silicon electrode can provide a lower irreversible capacity and higher efficiency.

Figure 8 compares the changes in the surface morphologies between the bare silicon electrode (S0) and the silicon electrode partially coated with DLC film (S4) before and after the electrochemical test. In the case of the bare silicon electrode, many cracks appeared on the electrode surface after the 40th cycle due to the severe volume change. However, the DLC-coated silicon electrode shows relatively small cracks, and a significant amount of active silicon remained on the electrode even after the 40th cycle. This is

because the large volume change of the silicon film and the instability of the interface between the silicon and electrolyte can be relieved by the DLC film [19–21]. These results suggest that the presence of the DLC film plays an important role in protecting the electrode against the destruction of the silicon thin film.

Conclusions

In the present work, the deposition of a DLC film on a silicon thin film anode was carried out using the RF-PECVD technique. The electrochemical characteristics of the silicon based electrodes were investigated as a function of their surface-coating morphology. The partially coated silicon electrodes showed improved cycleability as well as a high reversible capacity of $\sim 3,700 \text{ mA h g}^{-1}$ with an initial coulombic efficiency of $\sim 90\%$. This enhanced cycle performance and high specific capacity are attributed to the presence of the DLC films on the silicon electrode. The DLC layer not only imparted electrochemical stability to the silicon electrode, but also acted as a protective layer against the liquid electrolyte. These well-dispersed DLC-coating regions are expected to provide a promising surface-coating morphology for silicon electrodes, thereby enabling them to exhibit improved electrochemical performance factors such as a low irreversible capacity and good cycling performance.

Acknowledgment This research was supported by a grant (code #05K1501-01920) from the Center for Nanostructured Materials Technology under the 21st Century Frontier R&D Programs of the Ministry of Science and Technology, Korea.

References

- Holzappel M, Buqa H, Hardwick LJ, Hahn M, Würsig A, Scheifele W, Novák P, Kötz R, Veit C, Petrat FM (2006) *Electrochim Acta* 52:973
- Baranchugov V, Markevich E, Pollak E, Salitra G, Aurbach D (2007) *Electrochem Commun* 9:796
- Zuo P, Yin G, Yang Z, Wang Z, Cheng X, Jia D, Du C (2009) *Mater Chem Phys* 115:757
- Wang Y, Lee JY, Chen BH (2004) *J Electrochem Soc* 151:A563
- Grigoriants I, Soffer A, Salitra G, Aurbach D (2005) *J Power Sources* 146:185
- Liu S, Li Q, Chen Y, Zhang F (2009) *J Alloys Compd* 478:694
- Hathard TD, Darn JR (2004) *J Electrochem Soc* 151:A838
- Choi NS, Yew KH, Lee KY, Sung M, Kim H, Kim SS (2007) *J Power Sources* 161:1254
- Lee KL, Jung JY, Lee SW, Moon HS, Park JW (2004) *J Power Sources* 129:270
- Yang J, Winter M, Besenhard JO (1996) *Solid State Ion* 90:281
- Lee SJ, Lee JK, Chung SH, Lee HY, Lee SM, Baik HK (2001) *J Power Sources* 97–98:191

12. Winter M, Besenhard JO (1999) *Electrochim Acta* 45:31
13. Ratnakumar BV, Smart MC, Surampudi S (2001) *J Power Sources* 97/98:137
14. Angus JC, Koidl P, Domitz S (1986) In: Mort J, Jansen F (eds) *Plasma deposited thin films*. Chemical Rubber, Florida
15. Clay KJ, Speakman SP, Morrison NA, Tomozeiu N, Milne WI, Kapoor A (1998) *Diamond Relat Mater* 7:1100
16. Yang WJ, Sekino T, Shim KB, Niihara K, Auh KH (2005) *Surf Coat Technol* 194:128
17. Nakazawa H, Mikami T, Enta Y, Suemitsu M, Mashita M (2003) *Jpn J Appl Phys* 42:L676
18. Nakahigashi T, Tanaka Y, Miyake K, Oohara H (2004) *Tribol Int* 37:907
19. Endo E, Yasuda T, Kita A, Yamaura K, Sekai K (2000) *J Electrochem Soc* 147:1291
20. Moon HS, Ji KS, Kim TJ, Cho WI, Yoon YS, Chung SH, Park JW (2001) *J Ceram Process Res* 2:165
21. Shim HT, Lee JK, Cho BW (2007) *Solid State Phenomena* 124–126:919
22. Arie AA, Song JO, Lee JK (2009) *Mater Chem Phys* 113:249
23. Salcedo WJ, Peres EE, Fernandez JR, Rubim JC (2004) *Vib Spectrosc* 36:135
24. Dowling DP, A hern MJ, Kelly TC, Meenan BJ, Brown NMD, O'Connor GM, Glynn TJ (1992) *Surf Coat Technol* 53:177
25. Hatada R, Baba K (1999) *Nucl Instrum Methods Phys Res Sect B* 148:655